Period Doubling and Other Complex Bifurcations in Non-Isothermal Chemical Systems

S. K. Scott and A. S. Tomlin

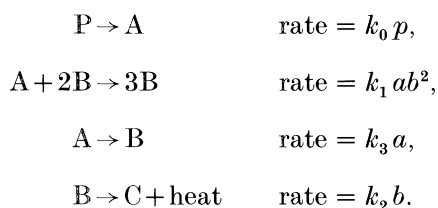|	
Email alerting service	Receive free email alerts when new articles cite this article - sign up in the box at the top right-hand corner of the article or click **here**

Period doubling and other complex bifurcations in non-isothermal chemical systems

By S. K. Scott and A. S. Tomlin

School of Chemistry, University of Leeds, Leeds LS2 9JT, U.K.

Chemical feedback in the form of chain-branching or autocatalysis can give rise to oscillatory behaviour in very simple models involving only two variables. Many chemical reactions are also exothermic. This chemical heat release can give rise to self-heating and hence to thermal feedback, where the temperature varies as well as the concentrations. When chemical and thermal feedback are coupled, the range of responses that can be observed are increased dramatically. These features are demonstrated through the simple non-isothermal autocatalator scheme

$$P \rightarrow A \qquad \text{rate} = k_0 p,$$

$$A + 2B \rightarrow 3B \qquad \text{rate} = k_1 ab^2,$$

$$A \rightarrow B \qquad \text{rate} = k_3 a,$$

$$B \rightarrow C + \text{heat} \qquad \text{rate} = k_2 b.$$

At its simplest, the reaction can be steady or can show simple period-1 oscillations. More complex oscillations, with higher periodicity appear as the experimental conditions are varied, with period doubling, mixed-mode oscillations and aperiodicity (chemical chaos).
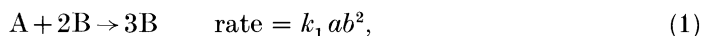
---

1. Introduction

Chemical reactions with two variables can exhibit multiple stationary-states and sustained oscillations in flow systems (Gray & Scott 1986). The oscillations in such systems are always simple, period-1 solutions. After transients have decayed each excursion has exactly the same period and amplitude as the next. There is a growing body of experimental evidence in chemistry for most complex, higher-order periodic (bursting) patterns and even aperiodic (chaotic) states. Examples include the solution-phase Belousov-Zhabotinsky reaction (Argoul *et al.* 1987; Hudson & Mankin 1981; Hudson & Rössler 1984; Maselko & Swinney 1986; Schmitz *et al.* 1977; Sørensen 1974), gas-phase combustion systems (Gray *et al.* 1981*a, b*, 1987), heterogeneous catalysis (Chang 1986; Jaeger *et al.* 1986; Möller *et al.* 1986; Wicke & Onken 1986) and electrodissolution reactions (Albahadily *et al.* 1989; Bassett & Hudson 1988, 1989; Lev *et al.* 1988; Schell & Albahadily 1989).

These more complex waveforms cannot arise with only two variables, but are characteristic of many three-variable systems. In this paper we examine at least some of the generic bifurcations in three-variable schemes, again exploiting a simple

4-2

model based on cubic autocatalysis. We study a thermodynamically closed reactor with no exchange of mass to the surroundings. Species A and B are intermediates in the conversion of a relatively stable reactant P to a final product C. The model scheme is

$$P \rightarrow A \qquad \text{rate} = k_0\,p, \tag{0}$$

$$A + 2B \rightarrow 3B \qquad \text{rate} = k_1\,ab^2, \tag{1}$$

$$A \rightarrow B \qquad \text{rate} = k_3\,a, \tag{3}$$

$$B \rightarrow C \qquad \text{rate} = k_2\,b. \tag{2}$$

(The numbering is chosen for consistency with Gray *et al.* (1987).) As well as the initial reaction in which species A is produced from the first-order decay of the precursor, an additional uncatalysed conversion of A to the autocatalyst B has been included in the model. The implications of this isothermal scheme have been reviewed in detail elsewhere (Merkin *et al.* 1986).

Oscillations in such a system will only be transient. However, with the so-called pool chemical approximation, the concentration of the reactant P is assumed to be large and to vary only slowly. We will return to this later, but with the approximation $p = p_0 = \text{const.}$, the model has just two independent concentrations, a and b. The pool chemical approximation also allows this system to have time-independent stationary state and sustained oscillatory solutions, and allows the techniques of local stability and Hopf bifurcation analysis to be applied directly.

Most spontaneous chemical reactions are to some extent exothermic (there are, of course, important exceptions to this statement). Similarly, most experimental apparatus does not have perfect heat transfer, so it is reasonable to assume that there may be some self-heating of the reacting mixture caused by the chemical heat release. The rates of chemical reactions are frequently sensitive to the local temperature and reaction rate 'constants' often show an Arrhenius temperature dependence $k = A\,e^{-E/RT}$. We shall therefore extend the isothermal system to a three variable system where the temperature excess will be the third variable. The extra coupling of thermal effects will be seen to have a dramatic effect on the dynamical behaviour of the system in some situations.

Rather than attempting the most general description, assigning an exothermicity to each reaction step and allowing all four rate constants to be temperature dependent, we look for the simplest extension. In reaction schemes involving reactive intermediates, the most significantly exothermic are the 'termination steps' such as step (2) above. The most highly temperature sensitive are those with the highest activation energy; initiation steps such as (0). Thus, here we assume step (2) is exothermic with $Q = -\Delta H > 0$ and k_0 has an Arrhenius form.

2. Governing equations, dimensionless quantities and the pool chemical approximation

The reaction rate equations for the concentrations of the three species P, A and B are

$$\mathrm{d}p/\mathrm{d}t = -k_0\,p, \tag{4}$$

$$\mathrm{d}a/\mathrm{d}t = k_0\,p - k_1\,ab^2 - k_3\,a, \tag{5}$$

$$\mathrm{d}b/\mathrm{d}t = k_1\,ab^2 + k_3\,a - k_2\,b. \tag{6}$$

When we wish to include the effects of the reaction exothermicity, we allow $k_0 = k_0(T)$ and also require the heat balance equation

$$V c_p c_0 \, \mathrm{d}T/\mathrm{d}t = V Q k_2 b - \chi S(T - T_{\mathrm{a}}). \tag{7}$$

Here V is the reactor volume, c_p the molar heat capacity, c_0 the molar density, χ the surface heat transfer coefficient, S the surface area and T_{a} the temperature of the surroundings to which heat is transferred by newtonian cooling: the difference $\Delta T = T - T_{\mathrm{a}}$ represents the temperature excess or degree of self-heating.

(a) Dimensionless quantities

For the flow reactor model in the previous paper, a natural measure of concentration presented itself: the inflow concentration of species A. This could then be combined with the autocatalytic rate constant k_1 to produce a natural chemical timescale. To follow a similar route here, we need again to find some appropriate measure of concentration, and also will need a natural temperature scale.

In a typical experiment, we might consider an initial state of pure P (or a solution of P) with some initial concentration p_0. Using p_0 as our base for concentration, p/p_0 will decay slowly from unity. If, however, A and B are reactive intermediates, their concentrations will typically remain many orders of magnitude lower than p_0. Thus a/p_0 and b/p_0 will always be very small quantities. Also, the chemical timescale given by $1/(k_1 p_0^2)$ will be very short, so our dimensionless time $k_1 p_0^2 t$ will have large values.

A more appropriate choice can be formed from the reaction rate constants for the competing autocatalyst production and removal steps (1) and (2). k_1 is a (pseudo) third-order rate constant so has units of concentration^{-2} s^{-1}, whereas the first-order k_2 has units of s^{-1}. The quotient $(k_2/k_1)^{\frac{1}{2}}$ therefore has units of concentration and we take this as our reference c_{ref}. Thus we have three dimensionless concentrations:

$$\pi = p/c_{\mathrm{ref}} = (k_1/k_2)^{\frac{1}{2}} p, \quad \alpha = a/c_{\mathrm{ref}} = (k_1/k_2)^{\frac{1}{2}} a, \quad \text{and} \quad \beta = b/c_{\mathrm{ref}} = (k_1/k_2)^{\frac{1}{2}} b. \tag{8}$$

We shall see that this choice is indeed appropriate as α and β will be of order unity in the parameter ranges of interest. As argued above, π will be a large quantity because p is typically orders of magnitude greater than c_{ref}.

Using the same reference concentration for the chemical timescale we find $t_{\mathrm{ch}} = 1/(k_1 c_{\mathrm{ref}}^2) = k_2^{-1}$, i.e. the autocatalyst decay reaction provides the natural timescale on which to judge slow or fast processes. Thus we take

$$\tau = k_2 t, \quad \kappa_u = k_3/k_2 \quad \text{and} \quad \kappa_0 = k_0/k_2, \tag{9}$$

where κ_u and κ_0 are dimensionless rate constants for the uncatalysed and reactant decay steps. If the latter are to be relatively slow processes then $\kappa_u, \kappa_0 \ll 1$. We may also remember that κ_0 is a function of temperature in the non-isothermal model.

To cope with the effects of self-heating, we may recast the heat balance equation in terms of the temperature excess ΔT rather than the absolute temperature itself. To make this dimensionless we can use the form most appropriate in thermal explosion theory and scale ΔT by RT_{a}^2/E to give $\theta = E\Delta T/RT_{\mathrm{a}}^2$. With this and introducing c_{ref} and t_{ch}, two final dimensionless quantities emerge:

$$\delta = Q c_{\mathrm{ref}} E/c_p c_0 RT_{\mathrm{a}}^2$$

is a dimensionless adiabatic temperature rise based on the reference concentration

and; $\gamma = \chi S / k_2 V c_p c_0$ is a dimensionless newtonian cooling coefficient. The actual maximum temperature rise in any given system is related to the initial concentration of reactant P and is given by $\theta_{ad} = \delta \pi_0$.

With these various forms, the reaction rate and heat balance equations become

$$\mathrm{d}\pi/\mathrm{d}\tau = -\kappa_0(\theta)\,\pi, \tag{10}$$

$$\mathrm{d}\alpha/\mathrm{d}\tau = \kappa_0(\theta)\,\pi - \alpha\beta^2 - \kappa_u\,\alpha, \tag{11}$$

$$\mathrm{d}\beta/\mathrm{d}\tau = \alpha\beta^2 + \kappa_u\,\alpha - \beta, \tag{12}$$

$$\mathrm{d}\theta/\mathrm{d}\tau = \delta\beta - \gamma\theta. \tag{13}$$

The form $\kappa_0(\theta)$ emphasizes the temperature dependence of the initiation process. For the Arrhenius rate-law we have this explicitly as

$$\kappa_0(\theta) = \kappa_{0,\mathrm{a}} \exp\{\theta/(1+\epsilon\theta)\}, \tag{14}$$

where $\kappa_{0,\mathrm{a}}$ is the value of κ_0 with k_0 evaluated at the ambient temperature and $\epsilon = RT_{\mathrm{a}}/E$.

Equations (10)–(14) are almost in the form we shall use, but some further reduction is appropriate as we see below. The initial conditions for the system are

$$\pi = \pi_0, \quad \alpha = \beta = 0 \quad \text{at} \quad \tau = 0. \tag{15}$$

(b) Orders of magnitude

As stated above, the choices of dimensionless groups ensure that α and β remain of order unity for 'interesting' parameter values. The dimensionless reactant concentration π is a large quantity initially, $\pi_0 \gg 1$. However, π only occurs in the governing equations multiplied by the parameter $\kappa_{0,\mathrm{a}}$: this is the dimensionless rate constant for the initiation step and will be small for a slow decay, i.e. $\kappa_{0,\mathrm{a}} \ll 1$. Thus the product $\kappa_{0,\mathrm{a}}\pi$ may be of order unity during the initial stages of the reaction and we replace this by the new dimensionless parameter $\mu = (k_0^2 k_1/k_2^3)^{\frac{1}{2}} p$. Equation (10) then becomes

$$\mathrm{d}\mu/\mathrm{d}\tau = -\kappa_0(\theta)\,\mu, \tag{16}$$

with $\mu = \mu_0$ at $\tau = 0$. Notice that the right-hand side is still multiplied by the small parameter κ_0. Provided we are dealing with systems that do not have high extents of self-heating, and κ_0 does not increase much beyond $\kappa_{0,\mathrm{a}}$ at any stage, we may apply the 'pool chemical approximation' to this form of the dimensionless reactant concentration. As long as μ_0 stays of order unity as $\kappa_{0,\mathrm{a}}$ tends to zero, we can take in this limit

$$\mu = \mu_0 = \text{const.} \tag{17}$$

Physically, we are neglecting reactant consumption: this clearly cannot hold for long times, but is appropriate with the above conditions for early dimensionless times, $\tau \approx O(\kappa_{0,\mathrm{a}}^{-1})$.

If we substitute for μ_0 into equation (11) we obtain

$$\mathrm{d}\alpha/\mathrm{d}\tau = \mu_0 \exp\{\theta/(1+\epsilon\theta)\} - \alpha\beta^2 - \kappa_u\,\alpha. \tag{18}$$

The Arrhenius temperature dependence here is a highly nonlinear, and somewhat awkward, form and there is much advantage in simplifying it where possible. If

the initiation step has a reasonably high activation energy, say 80 kJ mol^{-1} and $T_a = 300$ K, the group ϵ will be rather small, $\epsilon \approx 10^{-3}$. Provided the dimensionless temperature excess does not become large, the product $\epsilon\theta$ in the exponential argument will remain small compared with unity in the denominator. We can thus invoke the 'exponential approximation' replacing $\exp\{\theta/(1+\epsilon\theta)\}$ by e^θ. Elsewhere Gray & Kay (1990) use an alternative reduction, appropriate to situations where θ itself always remains small compared with unity. They replace the Arrhenius exponential with a linear term $\mu(1+\delta\theta)$. This also leads to important results and we discuss their implications later.

(c) *Dimensionless equations*

With the various reductions and approximations detailed above, the governing equations for the concentrations of A and B and for the temperature excess become

$$d\alpha/d\tau = \mu_0 e^\theta - \alpha\beta^2 - \kappa_u \alpha, \tag{19}$$

$$d\beta/d\tau = \alpha\beta^2 + \kappa_u \alpha - \beta, \tag{20}$$

$$d\theta/d\tau = \delta\beta - \gamma\theta. \tag{21}$$

Chemistry is coupled to the temperature through the heat release term $\delta\beta$ in equation (21) and the self-heating feeds back to the kinetics by 'forcing' the initiation step P $\to$ A. The classic two variable autocatalator can be derived as a special case of this more general three-variable scheme.

Two such limiting cases, with similar mathematical consequences, can be encapsulated in the limit $\gamma/\delta \to \infty$. Large values for the newtonian cooling coefficient imply either slow chemistry (k_2 small) or a high heat transfer coefficient χ or surface to volume ratio. Perhaps more realistic is the limit $\delta \to 0$, which implies a low specific exothermicity compared with a high specific heat capacity, such as pertains in dilute aqueous solutions. In these cases any initial temperature excess decays quickly and θ generally remains close to zero for all remaining times. (This is not always true for large γ when the above limit can be satisfied even when δ is not small: then there can be significant transient temperature excursions.)

Because we intend to look at low exothermicities where the temperature excess θ will remain small, we shall rescale θ in equations (19)–(21) and define a new variable $\phi = \theta/\delta$. The scheme now becomes

$$d\alpha/d\tau = \mu_0 e^{\delta\phi} - \alpha\beta^2 - \kappa_u \alpha, \tag{22}$$

$$d\beta/d\tau = \alpha\beta^2 + \kappa_u \alpha - \beta, \tag{23}$$

$$d\phi/d\tau = \beta - \gamma\phi. \tag{24}$$

Reduction to the two variable scheme is now automatic as $\delta \to 0$ and $e^{\delta\phi} \to 1$.

3. Stationary states and Hopf bifurcations for isothermal reaction scheme

Before proceeding with the analysis of the full three-variable system it is worth summarizing the responses of the simpler two-variable kinetic model in the absence of temperature effects (Merkin *et al.* 1986, 1987). We shall see that the latter provides an excellent first guide to the former in the important experimental situation where only small extents of self-heating are likely.
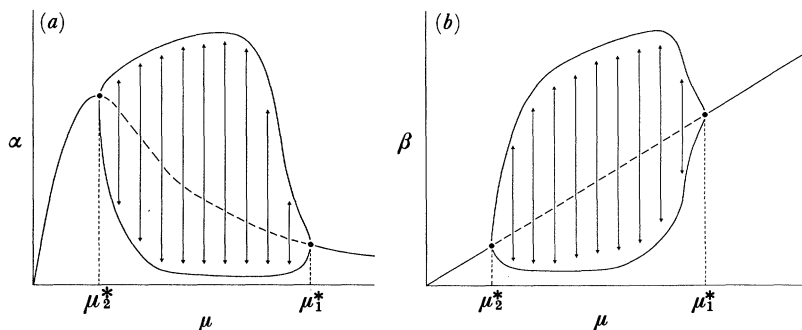
Figure 1. Steady-state profiles showing the variation of α and β with μ the bifurcation parameter. Also shown are the Hopf bifurcation points and the locus of limit cycles which emerge. At the value of κ_u chosen ($\kappa_u = 1.0 \times 10^{-3}$) the locus forms a 'canard' shape.

The classic, two-variable autocatalator is described by the coupled reaction rate equations

$$d\alpha/d\tau = \mu_0 - \alpha\beta^2 - \kappa_u \alpha, \tag{25}$$

$$d\beta/d\tau = \alpha\beta^2 + \kappa_u \alpha - \beta. \tag{26}$$

The stationary-state solutions for the isothermal system, equations (25) and (26) are given simply by

$$\alpha_{ss} = \mu/(\mu^2 + \kappa_u), \quad \beta_{ss} = \mu. \tag{27}$$

These forms are plotted as a function of the dimensionless reactant concentration (from which we have dropped the subscript for convenience) in figure 1 a, b. The concentration of species A shows a maximum of $\frac{1}{2}\kappa_u^{-\frac{1}{2}}$ at $\mu = \kappa_u^{\frac{1}{2}}$: the two loci cross for $\alpha_{ss} = \beta_{ss} = \mu = (1-\kappa_u)^{\frac{1}{2}}$. For a small value of the dimensionless uncatalysed reaction rate constant, the crossing occurs when the concentrations are close to unity, as we hoped with our scalings.

The stationary-state solution may become locally unstable for some range of μ. The upper and lower ends of this range are given by Hopf bifurcation points, $\mu_{1,2}^*$. Using the method from the previous paper, these are located as

$$(\mu_{1,2}^*)^2 = \frac{1}{2}\{1 - 2\kappa_u \pm (1 - 8\kappa_u)^{\frac{1}{2}}\}, \tag{28}$$

and these are real provided $\kappa_u < \frac{1}{8}$.

These points are marked in figure 1 for a particular choice, $\kappa_u = 1.0 \times 10^{-3}$ giving $\mu_1^* = 1.0 \times 10^{-3}$ and $\mu_2^* = 0.997$. Also shown is the evolution of the oscillatory amplitude in terms of the maximum and minimum attained by α and β on the corresponding limit cycle as a function of μ. An important feature here is the rapid growth in amplitude as μ decreases, slightly below the upper Hopf point: this is known as a 'canard'.

4. Three-variable scheme with self-heating

(a) Stationary states

The stationary-state solutions of equations (22)–(24) are given by

$$\phi_{ss} = \beta_{ss}/\gamma, \quad \alpha_{ss} = \beta_{ss}/(\beta_{ss}^2 + \kappa_u), \tag{29}$$
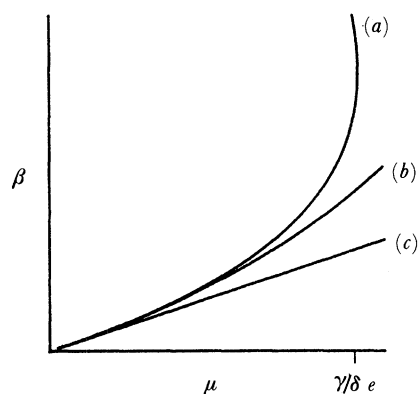
Figure 2. A comparison of the steady-state curves for the three models discussed in the text. (*a*) The exponential approximation $e^{\delta\theta}$ showing multistability; (*b*) the linear approximation of Gray & Kay (1990) $(1 + \delta\theta)$; (*c*) the two-variable isothermal model. Both the latter cases have a unique single steady state.

where β_{ss} is a solution of

$$\mu = \beta_{ss}\exp(-\delta\beta_{ss}/\gamma). \tag{30}$$

The stationary-state locus $\beta_{ss}(\mu)$ is shown in figure 2 in comparison with the linear relation (27) appropriate to the isothermal scheme and the curve $\beta_{ss} = \mu/[1 - (\delta\mu/\gamma)]$ for the Kay & Gray equations.

The non-isothermal scheme shows multiple stationary states for low μ and a thermal explosion as the reactant concentration increases: the latter corresponds to the turning point in the locus that occurs at $\mu = \gamma/\delta e$. For $\mu < \gamma/\delta e$, then, the system has one stationary state with $\beta_{ss} < \gamma/\delta$ and one with $\beta_{ss} > \gamma/\delta$. It is the lower of these two branches that is important to this study.

(*b*) *Local stability and Hopf bifurcation for three-variable systems*

The local stability of a given stationary state to infinitesimal perturbations is now determined by the three eigenvalues of the (3×3) jacobian matrix of equations (22)–(24) evaluated at that state. For the present scheme, the eigenvalues are given by the roots of the cubic equation

$$\lambda^3 + b\lambda^2 + c\lambda + d = 0, \tag{31}$$

where

$$b = 1 + \beta_{ss}^2 + \kappa_u + \gamma - 2\beta_{ss}^2/(\beta_{ss}^2 + \kappa_u): \quad c = (\beta_{ss}^2 + \kappa_u)(1 + \gamma) + \gamma - 2\gamma\beta_{ss}^2/(\beta_{ss}^2 + \kappa_u)$$

$$\text{and} \quad d = (\beta_{ss}^2 + \kappa_u)^2(\gamma - \delta\beta_{ss}). \tag{32}$$

If all three roots are negative or have negative real parts, the stationary state will be locally stable: if any has a positive real part the solution will be unstable.

On the upper branch of stationary states, $\delta\beta_{ss} > \gamma$ and so the coefficient d in equation (31) is negative. This means that one root must be real and positive. The upper branch consists of (unstable) saddle points.

On the lower branch, $\delta\beta_{ss} < \gamma$ and d is positive, so one real root is negative. The other roots may be real or form a complex pair. Hopf bifurcation requires the real
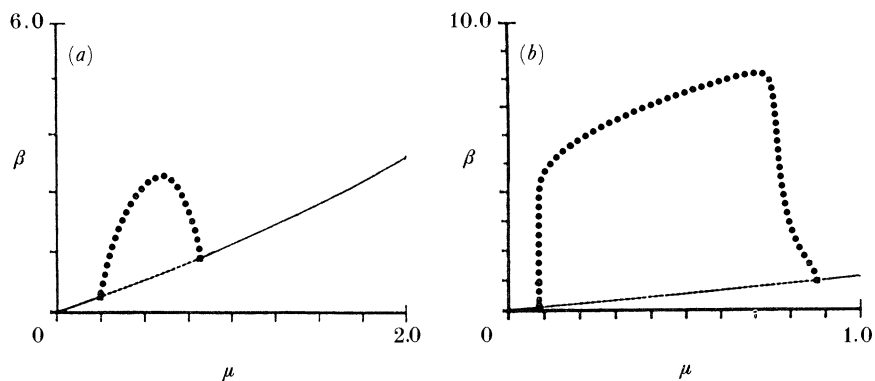
Figure 3. Bifurcation diagrams showing variation in maximum value of concentration β during oscillation with μ. In both cases $\gamma = 1.0, \delta = 0.1$: (a) $\kappa_u = 5.0 \times 10^{-2}$, small amplitude oscillations; (b) $\kappa_u = 7.0 \times 10^{-3}$ showing steeply rising amplitude close to the upper Hopf point and the 'canard' shape.
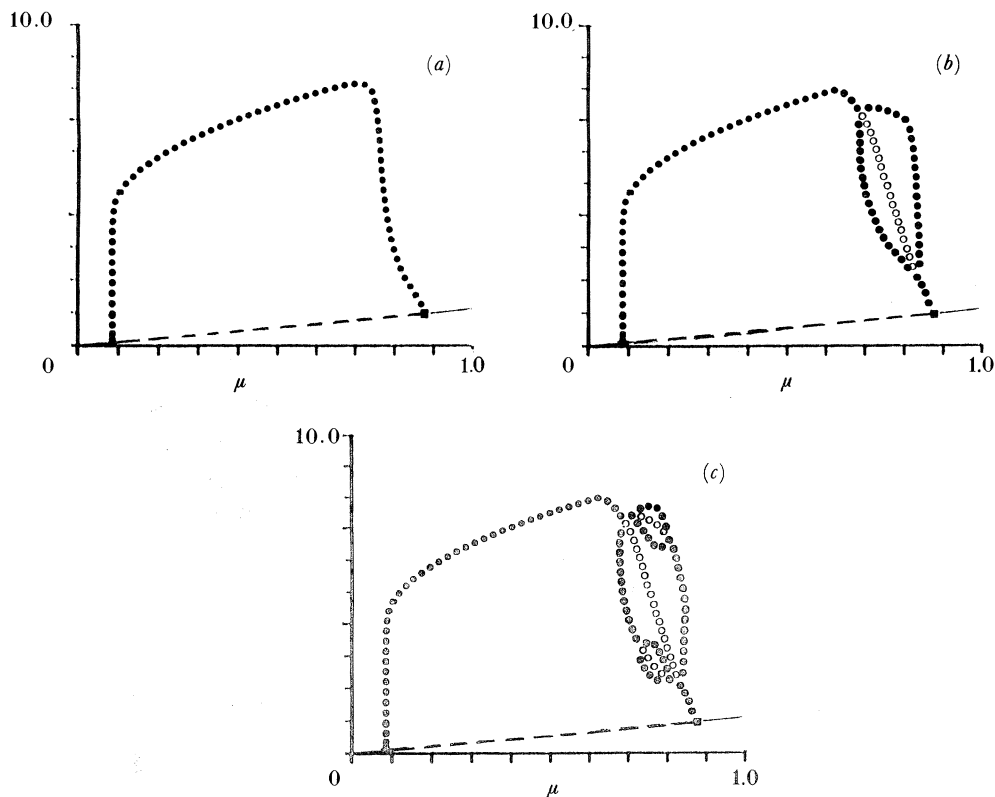

Figure 4. Bifurcation diagrams showing the appearance of 'bubbles' of higher and higher period oscillations as the heat transfer coefficient decreases. In all cases $\kappa_u = 5.5 \times 10^{-3}$ and $\delta = 0.1$. (a) $\gamma = 1.0$ showing a locus of simple period one oscillations; (b) $\gamma = 0.7$, a region of period-2 oscillations has now appeared for some values of μ; (c) $\gamma = 0.65$, further 'bubbles' of period-4 solutions have arisen and when γ reaches 0.5 a full cascade to chaos can be achieved.
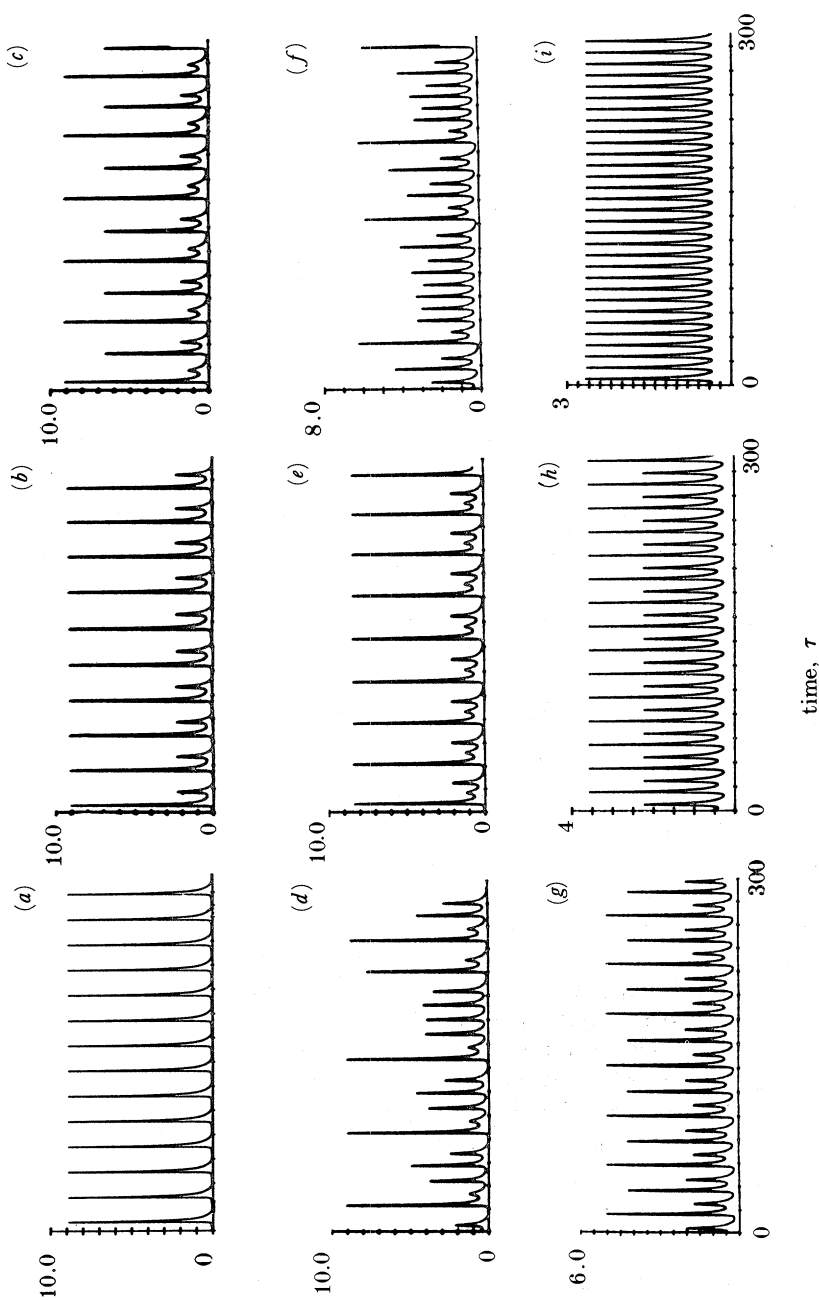
Figure 5. A series of time traces for $\gamma = 0.5$, $\delta = 0.1$, $\kappa_u = 5.5 \times 10^{-3}$ showing parts of the period doubling sequence leading to chaos. (*a*) $\mu = 0.6$, period-1 oscillations; (*b*) $\mu = 0.65$, period-2; (*c*) $\mu = 0.687$, period-4; (*d*) $\mu = 0.6887$, chaotic trace; (*e*) $\mu = 0.695$, a window of period-3 oscillations; (*f*) $\mu = 0.708$, smaller-amplitude chaotic trace; (*g*) $\mu = 0.71$, period-4, part of the reverse period-doubling cascade; (*h*) $\mu = 0.715$, period-2; (*i*) $\mu = 0.72$ return to simple low-amplitude period-1 oscillations.

part of such a complex pair to pass through zero. In terms of the coefficients in equation (31) this condition can be expressed as

$$bc = ad, \tag{33}$$

with $d > 0$.

Although equations (32) and (33) cannot be combined to give any useful analytical result in general, limiting forms can be established. In the isothermal limit, $\delta \to 0$, the cubic equation factorizes to give $\lambda = -\gamma$ and the quadratic appropriate to the isothermal scheme of §3. The condition for Hopf bifurcation is then given by equation (28). So for small δ this can be used as a good approximation to the Hopf condition for the non-isothermal scheme.

For $\kappa_u = 0$ (no uncatalysed step), the upper Hopf point lies below the saddle-node turning point only if

$$\delta < [\gamma(1+\gamma)]^{\frac{1}{2}}. \tag{34}$$

This gives a good guide to the conditions where two Hopf points exist in the case where κ_u is small.

In general, however, we rely on computational methods to determine the Hopf points μ^* for a given set of parameters $(\kappa_u, \delta, \gamma)$. Using the path-following routine AUTO (Doedel 1986) we can also follow the emerging oscillatory solutions. In all cases the Hopf bifurcations are supercritical. The limit cycles that emerge will therefore be stable in the regions close to the bifurcation points. In certain parameter ranges, however, the limit cycle between two Hopf points can become unstable. These instabilities can arise in several ways and path-following techniques can be used to locate these further bifurcations.

5. Oscillatory solutions and their development

(a) Simple periodic solutions

We have stated in the previous section that it is possible to have zero, one or two Hopf bifurcation points in our bifurcation diagram. The results in this section will be concerned with the latter of these cases: that which involves two Hopf points with a region of stationary-state instability between them. Oscillatory solutions emerge from these bifurcations and path following enables their behaviour to be followed away from the Hopf points. The simplest case has a stable period-1 solution across the whole region between the two Hopf bifurcations. Choosing a relatively large value for κ_u, the rate for the uncatalysed step, the locus of limit cycles forms an egg shape in the β–γ plane. An example of these limit cycles in figure $3a$ is for $\gamma = 1.0$, $\delta = 0.1$ and $\kappa_u = 5.0 \times 10^{-2}$. At lower uncatalysed reaction rates, e.g. for $\kappa_u = 7.0 \times 10^{-3}$ (figure $3b$), the locus develops a 'canard'. When we come to study more complex dynamics in the following sections we will discover that it is these smaller values of κ_u that are the most interesting. The bifurcations to higher-period oscillations will be seen to occur in the region of steeply rising amplitude below the upper Hopf point.

(b) Period-doubling sequences and 'bubbling' patterns

In this section we shall look at the influence of the heat transfer parameter γ on the dynamics of the system. If we choose the parameter values $\kappa_\mu = 5.5 \times 10^{-3}$, $\delta = 0.1$ and $\gamma = 1.0$ we see a series of limit cycles forming a canard shape, figure $4a$, similar to that seen in the isothermal system. These limit cycles represent simple period-1 oscillations. For smaller values of γ, corresponding to slower heat loss, this
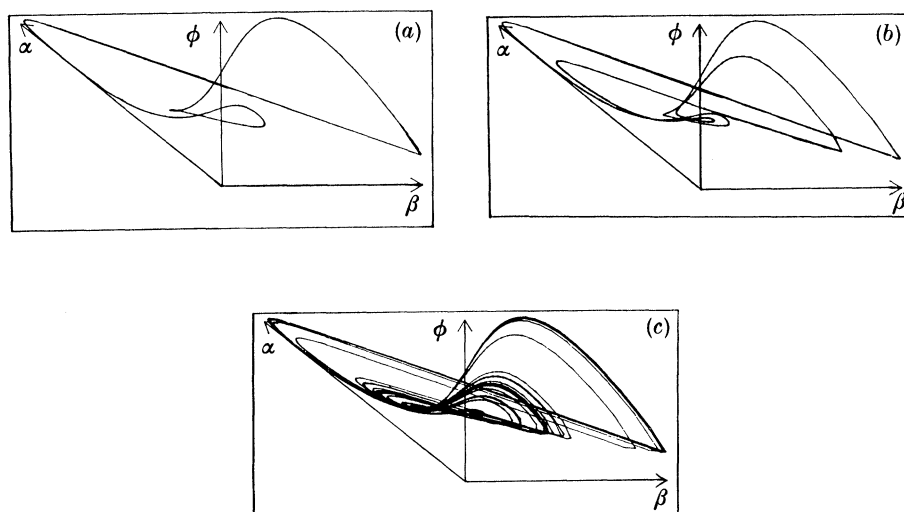
Figure 6. Three-dimensional diagrams of the attractors and limit cycles corresponding to the traces in figure 5. (a) $\mu = 0.65$, period-2 limit cycle; (b) $\mu = 0.687$, the period-2 limit cycle has gradually split to form a period-4 attractor; (c) $\mu = 0.695$, a chaotic attractor showing the characteristic folding feature. Notice that the attractor is not fully three dimensional but is locally planar in nature.

branch of limit cycles becomes unstable for certain values of the bifurcation parameter μ. With $\gamma = 0.7$ a pair of period-doubling bifurcations has appeared and a branch of period-2 oscillations exists between them as shown in figure 4b. The maximum amplitude of the peaks is no longer repeated every oscillation, but every two oscillations.

Decreasing γ further to 0.65 we see the period-2 oscillations bifurcate by period doubling, and a branch of period-4 oscillations appears (figure 4b). The bifurcation diagrams now show clearly the appearance of 'bubbling' patterns. For this value of γ, as we change the precursor concentration μ we shall see a sequence of oscillations of the following kind:

period 1 – period 2 – period 4 – period 2 – period 1.

More and more of these bubbles with higher periodic solutions appear as γ is decreased further, and by $\gamma = 0.5$ a full cascade to chaotic oscillations has been achieved. This period doubling cascade is a well-documented route to chaotic behaviour and is seen in many dynamical systems (Feigenbaum 1980). The time traces in figure 5a–c show part of the period doubling sequence leading to a chaotic trace (d) on increasing μ. This is followed by a reverse period doubling sequence at higher reactant concentrations, figure 5g–i, returning to (small amplitude) period-1.

Figure 6 shows how the limit cycle splits as the period doubles and shows the typical folding and locally planar characteristics of the chaotic attractor produced. Another feature of such chaotic regions is the appearance of periodic windows. In figure 5e we see that a window of period-3 oscillations appears at $\mu = 0.696$, a parameter value within the chaotic band. Other periodic windows will also exist but over much narrower parameter ranges and so will be more difficult to detect. Figure 7 shows a successive maxima plot for the chaotic attractor. This is produced by
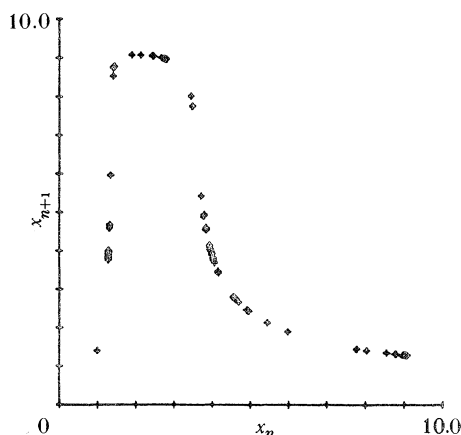
Figure 7. Next maxima plot of x_{n+1} against x_n, for β that corresponds to the chaotic attractor shown in figure 6.

plotting the maximum value of β for each peak in the time trace against the previous maximum. The points gradually fill out a humped shape map. This map is a characteristic feature of such a chaotic attractor.

(c) *Mixed-mode oscillations*

For certain parameter values the simple period-1 limit cycle found in this model can lose stability in another way. This is by a bifurcation to 'mixed mode' oscillations. By the term 'mixed mode' we mean a solution which is a combination of large-amplitude relaxation type oscillations and any number of small oscillations separating the large excursions. A sequence of time traces of these kind of oscillations is shown in figure 8. They have also been seen in many experimental situations, such as the Belousov-Zhabotinsky reaction and the spontaneous oxidation of hydrogen.

If we study the sequence shown in figure 8, we see that as the bifurcation parameter μ is increased, the number of small-amplitude oscillations between each large peak increases. This kind of progression has been noted in experimental situations. Eventually when μ is increased to a value of 0.5586, the number of small peaks between each large one no longer remains constant. A chaotic attractor has been formed although it is of a different nature to the one in the previous section. A further increase in μ will result in the disappearance of the large peaks altogether and a small amplitude attractor will be left behind which is still aperiodic. Periodicity returns for larger μ, with period-1 traces reappearing at the end of a reverse period doubling sequence similar to the one shown in figure 5. Another feature of these sequences of mixed-mode oscillations, is that as the number of small oscillations between the large peaks increases, the parameter regions in which they are found become narrower. Thus the region with alternate small and large peaks will be more easily found than the region with say one large and three small peaks.

To understand the kind of trajectory which we see in this region of complex oscillations, it will be helpful to refer back to the two variable model. As discussed previously if we let $\delta \to 0$ then the temperature variable ϕ or θ becomes decoupled from the concentrations. For values of μ between the two Hopf points of the corresponding isothermal system, α and β still oscillate. If we choose μ to be close to
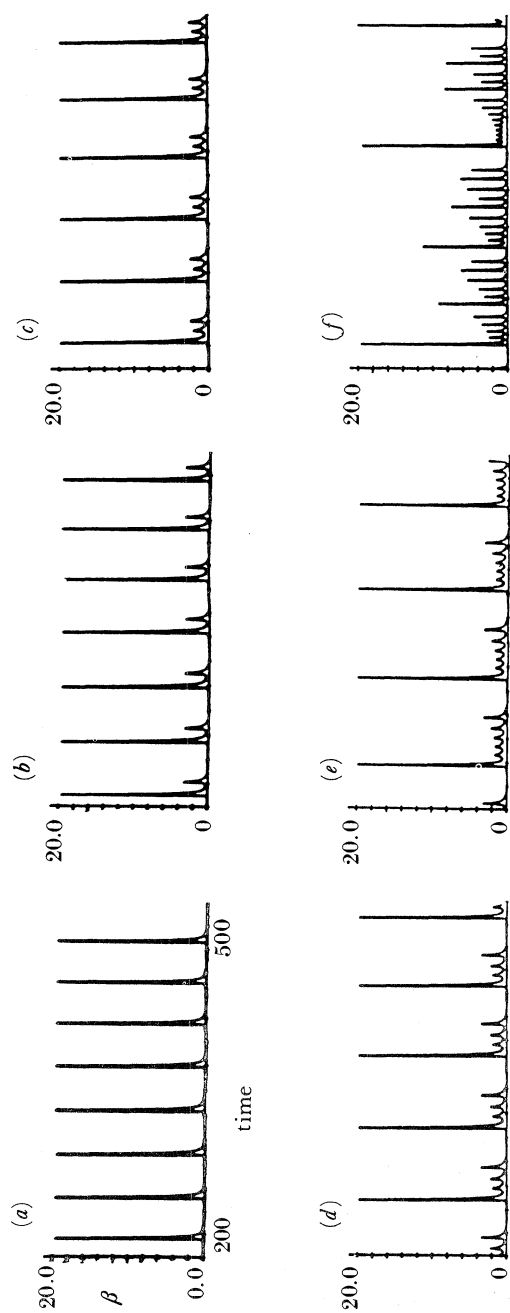
Figure 8. A sequence of oscillations in the 'mixed-mode' region showing how the number of small amplitude oscillations increases as μ increases. $\gamma = 0.05$, $\delta = 0.025$, $\kappa_u = 1.0 \times 10^{-3}$. (a) $\mu = 0.498$, small-amplitude period-1; (b) $\mu = 0.51$; (c) $\mu = 0.53$; (d) $\mu = 0.535$; (e) $\mu = 0.55$; (f) $\mu = 0.5586$ large-amplitude chaotic trace.
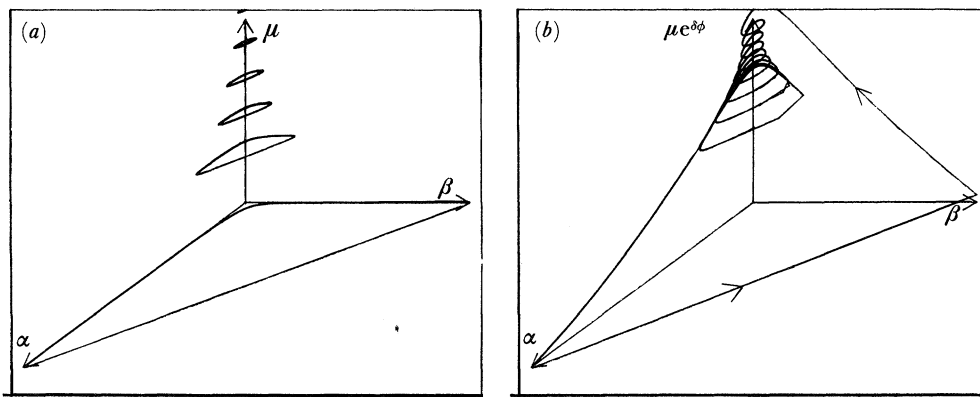
Figure 9. Responses in the $\mu\,e^{\delta\phi}-\alpha-\beta$ plane with $\gamma = 0.05$, $\kappa_u = 1.0 \times 10^{-3}$. (a) Limit cycles for the isothermal system, $\delta = 0$, for values of μ between 0.85 and 1.0; (b) the full three-dimensional system with $\delta = 0.025$ and $\mu = 0.558$, showing the corresponding spiral attractor with $\mu\,e^{\delta\phi}$ oscillating between approximately 0.85 and 1.0.
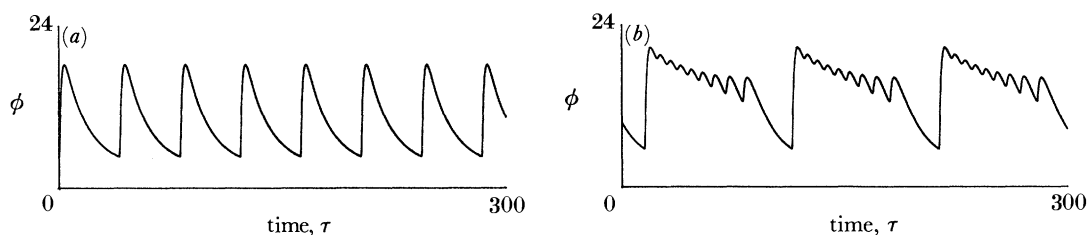

Figure 10. Evolution of dimensionless temperature excess ϕ for $\gamma = 0.05$, $\kappa_u = 1.0 \times 10^{-3}$ and $\mu = 0.558$. (a) 'Isothermal' case with ϕ decoupled showing sharp rise and almost exponential decay; (b) the exponential decay is altered when the temperature excess is recoupled into the system with $\delta = 0.025$.

the upper Hopf point, then the amplitude of the oscillations will be small. As the value of μ is decreased then the limit cycle will grow in a canard shape as shown earlier. Away from the Hopf point the amplitude will begin to increase quickly until large oscillations are reached (Merkin *et al.* 1987). A sequence of these limit cycles for various values of μ is shown in figure 9a. The dimensionless temperature excess ϕ also oscillates, driven by β with some phase-lag, but does not feedback to the chemistry. Figure 10a shows a typical temperature trace for $\mu = 0.558$: ϕ increases sharply and then decays exponentially during each oscillation.

To illustrate the influence of the temperature effect on the full scheme we consider recoupling ϕ by allowing δ to increase from zero, still with $\mu = 0.558$, which lies within the mixed mode region. By recoupling the equations what we are effectively doing is replacing the parameter μ in the decoupled system by the term $\mu\,e^{\delta\phi}$. We are adding an internal forcing to the system. The terms ϕ and, equivalently, $\mu\,e^{\delta\phi}$ no longer show a simple exponential decay in each oscillation. This time as $\mu\,e^{\delta\phi}$ decays it effectively winds around the limit cycles in figure 9a. We now see a spiral-shaped attractor in three dimensions, and an example of this is shown in figure 9b.

When $\mu\,e^{\delta\phi}$ reaches a low enough value then the limit cycle becomes large again.
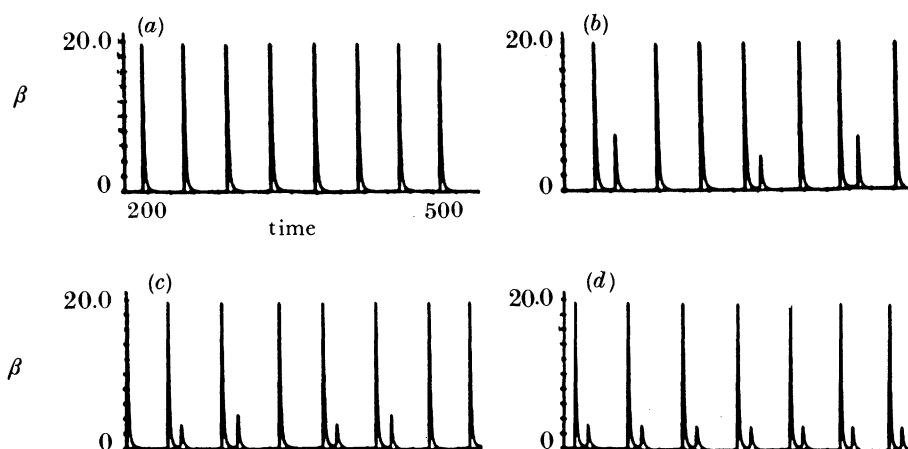
Figure 11. More complex patterns found in the 'mixed-mode' region. $\gamma = 0.05$, $\delta = 0.025$, $\kappa_u = 1.0 \times 10^{-3}$. (a) $\mu = 0.50$; (b) $\mu = 0.505$; (c) $\mu = 0.51$.

A sharp peak in β then causes ϕ to increase very sharply and the trajectory moves away from its stable manifold. The effective initiation rate $\mu e^{\delta\phi}$ is driven up to its maximum value from which it begins to spiral down again. Figure 9 a, b shows a very good correspondence between the size of the limit cycles in the two variable case and the size of the spirals in the non-isothermal system. Obviously the lower the value of μ in the three-variable system, the lower the maximum value of $\mu e^{\delta\phi}$ will be. This means that the trajectory will pass through fewer spirals as $\mu e^{\delta\phi}$ decays. Here we have some indication as to why the number of small peaks between each large one increases with increasing μ.

On first glance at this complex region it would seem that the period of oscillations increases gradually with μ, in direct contrast with the period doubling case. However, if we take a close look at the regions between each simple period oscillation we find even more complications. For example, if we study the region between the period-1 and the period-2 patterns we find a mixture of the two states. Figure 11 shows an example of these more complex concatenations. In figure 11 b we have three large oscillations followed by a small peak and then two large ones followed by a small peak. Similar complexities appear between each of the other simpler periodic patterns although over much smaller parameter regions.

We see that the period of the oscillations does not vary in a simple way as first appeared. The more complex patterns have a larger repeating group and therefore a longer period than the simple ones. However, even considering these complex patterns we still see an increasing number of small oscillations per large peak as we follow a sequence. If we calculate the ratio of small to large peaks we find that it increases in a stepwise manner as the bifurcation parameter increases.

Discussion and Conclusions

We have seen how an isothermally oscillating chemical reaction can be perturbed by a second feedback system. In this particular example we have considered a thermal effect as the source of this feedback, but in general this could also be

Phil. Trans. R. Soc. Lond. A (1990)

provided by chemical autocatalysis or inhibition (Hudson & Rössler 1984). Gray & Aarons (1974) considered a one-variable chemical model and showed that small temperature variations there could produce what they termed 'parasitic oscillations'. In the present model, the self-heating leads to complex oscillations and parasitic chaos. The amount of self-heating required to produce these complexities need not be large, as we shall see.

We can estimate the actual magnitude of the temperature excursions in the following way. In terms of our variables, the degree of self-heating is given by $\Delta T = \theta R T_a^2/E = \delta\phi R T_a^2/E$. For chemical systems at room temperature we have $T_a = 300$ K and may take a representative activation energy $E = 90$ kJ mol^{-1}. Taking a typical value for the dimensionless temperature excursion from figure 4, we see $\theta = \delta\phi = 0.1$. Thus the maximum temperature excess is less than 1 K for this example. In fact there is no reason to suppose there will be a minimum degree of self-heating capable of inducing complex oscillatory or aperiodic behaviour and this influence may well be too small to be detected directly. Nevertheless its effect can be observed as the chemistry acts in some sense as a (nonlinear) amplifier.

The feedback studied here has a nonlinear form μe^θ so as to mimic the chemical situation of an Arrhenius temperature dependence. As Gray & Kay (1990) show elsewhere, this nonlinearity is not required mathematically to produce complex traces. All of the oscillatory waveforms and sequences amongst them presented above, can be obtained with the simple linear coupling $\mu(1+\theta)$. In the latter case there is only a unique stationary state, which confirms that the saddle point solution (upper branch) in the present model does not have a determining influence on the changes in the oscillatory dynamics. In both cases, the observed three-dimensional behaviour can be immediately understood in terms of the underlying structure provided by the two-variable isothermal model. If the effective value of the initiation rate, i.e. μe^θ, is varying across a range for which the amplitude of the oscillation in the isothermal scheme is particularly sensitive to μ, i.e. near the canard, the resulting response will naturally have a mixed-mode character.

This link can be made formally by considering the governing equations for a weakly exothermic system with relatively slow heat transfer ($\delta, \gamma \ll 1$). Introducing the new parameters $\epsilon\Delta = \delta$ and $\epsilon\Gamma = \gamma$ where Δ and Γ are of order unity and $\epsilon \ll 1$, and a new (slow) timescale $T = \epsilon\tau$, equations (19)–(21) can be written in the form

$$\epsilon\, d\alpha/dT = \mu e^\theta - \alpha\beta^2 - \kappa_u \alpha,$$

$$\epsilon\, d\beta/dT = \alpha\beta^2 + \kappa_u \alpha - \beta$$

and
$$d\theta/dT = \Delta\beta - \Gamma\theta.$$

The appearance of the small parameter multiplying the derivatives $d\alpha/dT$ and $d\beta/dT$ means that for most of the evolution of the system the concentrations change on a faster timescale than the temperature excess, allowing the term μe^θ to be considered as a slowly varying parameter.

An alternative special case, also of practical interest, is that of a highly exothermic reaction competing with a high heat transfer coefficient ($\delta, \gamma \gg 1$). Now, using $\Delta = \epsilon\delta$ and $\Gamma = \epsilon\gamma$ with $\Delta, \Gamma \sim O(1)$ and $\epsilon \ll 1$, the governing equations have the form

$$d\alpha/d\tau = \mu e^\theta - \alpha\beta^2 - \kappa_u \alpha,$$

$$d\beta/d\tau = \alpha\beta^2 + \kappa_u \alpha - \beta$$

and
$$\epsilon\, d\theta/d\tau = \Delta\beta - \Gamma\theta.$$

Now the temperature is the fast variable. We can expect θ to adjust rapidly until

$$\theta = \Delta\beta/\Gamma = \delta\beta/\gamma,$$

so the temperature excess will closely follow the autocatalyst concentration. With these scalings we can expect the behaviour of the three-variable system to be closely related to the two-variable subscheme

$$d\alpha/d\tau = \mu\,e^{\delta\beta/\gamma} - \alpha\beta^2 - \kappa_u\alpha$$

and
$$d\beta/d\tau = \alpha\beta^2 + \kappa_u\alpha - \beta.$$

This model has successfully reproduced two of the common routes from periodic oscillations to chaos observed in many chemical (and other physical, engineering and biological) systems. One of these, the period-doubling sequence, is relatively familiar. The other is not easily characterized. It appears to have some of the hallmarks of intermittency (itself a rather ill-defined process) but not conclusively so. Other routes observed in other systems involve quasiperiodic responses corresponding to motion on a torus in the phase-plane. We have not found such behaviour in the present model over the parameter ranges investigated, but it may be relevant under other conditions.

Much of the analysis performed in this study has relied on the existence of stationary-state solutions or 'invariant attractors' such as limit cycles. These are somewhat artificial as they rely on the pool chemical approximation that effectively ignores reactant consumption. In fact we know that our thermodynamically closed system must tend irrevokably towards the corresponding state of chemical equilibrium, and that this must be a stable state. Eventually, therefore, all 'exotic' behaviour including even simple period-1 oscillations must die out. The different responses discussed in the previous sections may still be important, however. They will help determine the transient behaviour that accompanies this evolution from the initial conditions to the equilibrium state. The isothermal model with a decaying reactant concentration has been considered by Merkin *et al.* (1987). For the non-isothermal scheme here, the situation will be qualitatively similar although more complex. The reactant concentration no longer follows a simple exponential decay as the rate of step (0) now depends on the (varying) temperature. Selected computations with a slow reactant consumption included have been made and do indeed show the system traversing through complex time-dependent sequences characteristic of the sustained oscillations of the forms observed above.

References

Albahadily, F. N., Ringland, J. & Schell, M. 1989 *J. chem. Phys.* **90**, 813–821.

Argoul, F., Arneodo, A., Richetti, P., Roux, J.-C. & Swinney, H. L. 1987 *Acc. chem. Res.* **20**, 436–442.

Bassett, M. R. & Hudson, J. L. 1988 *J. phys. Chem.* **92**, 6963–6966.

Bassett, M. R. & Hudson, J. L. 1989 *J. phys. Chem.* **93**, 2731–2736.

Chang, H.-S. 1986 *Dynamics of nonlinear systems* (ed. V. Hlavacek), pp. 85–110. New York: Gordon & Breach.

Doedel, E. 1986 *Auto-continuation and bifurcation problems in ordinary differential equations.*

Feigenbaum, M. J. 1980 *Los Alamos Sci.* **1**, 4–28.

Gray, B. F. & Aarons, L. J. 1974 *Faraday Discuss. Chem. Soc.* **9**, 129–136.

Gray, P. & Kay, S. R. 1990 (In preparation.)

Gray, P., Griffiths, J. F., Hasko, S. M. & Lignola, P.-G. 1981*a* *Proc. R. Soc. Lond.* A **374**, 313–339.

Gray, P., Griffiths, J. F., Hasko, S. M. & Lignola, P.-G. 1981*b* *Combust. Flame* **43**, 175–186.

Gray, P., Griffiths, J. F., Pappin, A. & Scott. S. K. 1987 *Complex chemical reaction systems* (ed. J. Warnatz & W. Jäger), pp. 150–159. Berlin: Springer-Verlag.

Gray, P. & Scott, S. K. 1986 *Ber. BunsenGes. phys. Chem.* **90**, 985–996.

Hudson, J. L. & Mankin, J. C. 1981 *J. chem. Phys.* **74**, 6171–6177.

Hudson, J. L. & Rössler, O. E. 1984 *Modelling of patterns in space and time* (ed. W. Jäger & J. D. Murray), pp. 135–145. Berlin: Springer-Verlag.

Jaeger, N. I., Ottensmeyer, R. & Plath, P. J. 1986 *Ber. BunsenGes. phys. Chem.* **90**, 1075–1079.

Lev, O., Wolfberg, A., Sheintuch, M. & Pismen, L. M. 1988 *Chem. Engng Sci.* **43**, 1339–1353.

Maselko, J. & Swinney, H. L. 1986 *J. chem. Phys.* **85**, 6430–6441.

Merkin, J. H., Needham, D. J. & Scott, S. K. 1986 *Proc. R. Soc. Lond.* A **406**, 299–323.

Merkin, J. H., Needham, D. J. & Scott, S. K. 1987 *J. engng Maths.* **21**, 115–127.

Möller, P., Wetzl, K., Eiswurth, M. & Ertl, G. 1986 *J. chem. Phys.* **85**, 5328–5336.

Schell, M. & Albahadily, F. N. 1989 *J. chem. Phys.* **90**, 822–827.

Schmitz, R. A., Graziani, K. R. & Hudson, J. L. 1977 *J. chem. Phys.* **67**, 3040–3044.

Sørensen, P.-G. 1974 *Faraday Discuss. Chem. Soc.* **9**, 88.

Wicke, E. & Onken, H. U. 1986 *Chem. Engng Sci.* **41**, 1681–1687.